

Article

# Molecular Structure, Spectroscopic and DFT Computational Studies of Arylidene-1,3-dimethylpyrimidine-2,4,6(1*H*,3*H*,5*H*)-trione

Assem Barakat <sup>1,3,\*</sup>, Saied M. Soliman <sup>2,3,\*</sup>, Hazem A. Ghabbour <sup>4,5</sup>, M. Ali <sup>1</sup>,  
Abdullah Mohammed Al-Majid <sup>1</sup>, Mohammad Shahidul Islam <sup>1</sup> and Ayman A. Ghfar <sup>1</sup>

<sup>1</sup> Department of Chemistry, College of Science, King Saud University, P.O. Box 2455, Riyadh 11451, Saudi Arabia; maly.c@ksu.edu.sa (M.A.); amajid@ksu.edu.sa (A.M.A.-M.); shahid.10amui@gmail.com (M.S.I.); aymanghfar@gmail.com (A.A.G.)

<sup>2</sup> Department of Chemistry, Rabigh College of Science and Art, P.O. Box 344, Rabigh 21911, Saudi Arabia

<sup>3</sup> Department of Chemistry, Faculty of Science, Alexandria University, P.O. Box 426, Ibrahimia, Alexandria 21321, Egypt

<sup>4</sup> Department of Pharmaceutical Chemistry, College of Pharmacy, King Saud University, P.O. Box 2457, Riyadh 11451, Saudi Arabia; ghabbourh@yahoo.com

<sup>5</sup> Department of Medicinal Chemistry, Faculty of Pharmacy, Mansoura University, Mansoura 35516, Egypt

\* Correspondences: amarakat@ksu.edu.sa (A.B.); saied1soliman@yahoo.com (S.M.S.);  
Tel.: +966-11467-5884 (A.B.); +966-56545-0752 (S.M.S.); Fax: +966-11467-5992 (A.B.)

Academic Editor: Helmut Cölfen

Received: 4 July 2016; Accepted: 5 September 2016; Published: 8 September 2016

**Abstract:** Reaction of barbituric acid derivatives and di-substituted benzaldehyde in water afforded arylidene-1,3-dimethylpyrimidine-2,4,6(1*H*,3*H*,5*H*)-trione derivatives (**1** and **2**). The one step reaction proceeded efficiently, smoothly, and in excellent yield. The arylidene compounds were characterized by spectrophotometric tools plus X-ray single crystal diffraction technique. Quantum chemical calculations were performed using the DFT/B3LYP method to optimize the structure of the two isomers (**1** and **2**) in the gas phase. The optimized structures were found to agree well with the experimental X-ray structure data. The highest occupied (HOMO) and lowest unoccupied (LUMO) frontier molecular orbitals analyses were performed and the atomic charges were calculated using natural population analysis.

**Keywords:** green chemistry; barbituric acid; Density functional theory (DFT)-computation

## 1. Introduction

The barbituric acid scaffold and particularly the substituted derivatives at the C5-position are found as a core structure in many potential pharmaceutical drugs. Several examples of the arylidene derivatives of barbituric acid possessing significant implementation in the pharmaceutical field such as antitumor [1], immunomodulating, matrix metalloproteinase (MMP) inhibitor [2], antioxidant [3], antibacterial agent [4], anticonvulsant potentials [5], and mutant SOD1-dependent protein aggregation [6] were investigated. Additionally, these compounds were shown to have several targets in dye manufacturing [7], supramolecular chemistry [8], and in nonlinear optical study [9].

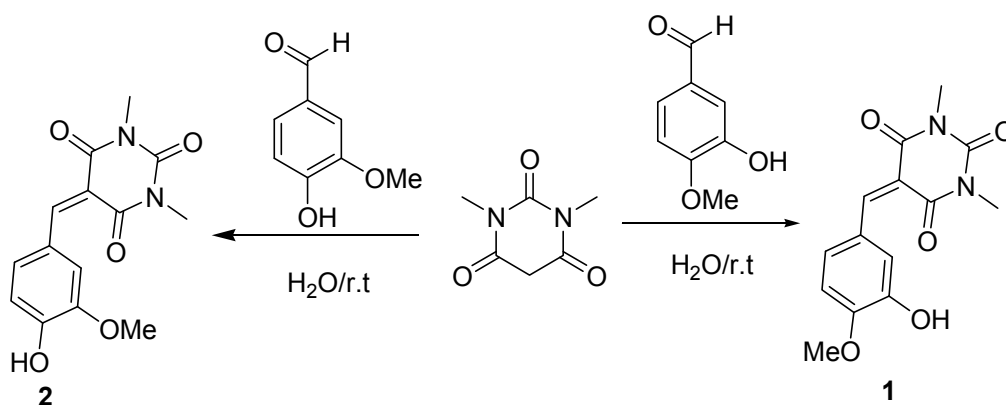
In green chemistry, water is the ideal solvent: it is non-toxic, benign, sustainable, non-flammable, has a high specific heat capacity to absorb energy from reactions, has a very low odor, and is available at a low cost [10]. Due to these advantages, a wide variety of chemical reactions can be performed in water. One of these reactions is the Aldol condensation that proceeds smoothly in water.

In continuation of our research program [11–17], we synthesized two new compounds from the reaction of barbituric acid derivatives and di-substituted benzaldehyde. Their 3D chemical structures were investigated by X-ray diffraction and computational studies.

## 2. Results

### 2.1. Chemistry

The arylidene-1,3-dimethylpyrimidine-2,4,6(1*H*,3*H*,5*H*)-trione derivatives **1** and **2** were synthesized as shown in Scheme 1. Barbituric acid derivatives, and 3-hydroxy-4-methoxybenzaldehyde (for the synthesis of **1**) or 4-hydroxy-3-methoxybenzaldehyde (for the synthesis of **2**) are commercially available. The reaction proceeds smoothly with the mixing of equimolar amounts of the substituted aldehyde and barbituric acid derivative in water at room temperature providing the arylidene compounds in excellent yield. The molecular structures of the later products were investigated by using different spectroscopic techniques such as  $^1\text{H}$ ,  $^{13}\text{C}$ -NMR, IR, GCMS, and the X-ray single crystal technique.



Scheme 1. Synthesis of arylidene-1,3-dimethylpyrimidine-2,4,6(1*H*,3*H*,5*H*)-trione derivatives **1** and **2**.

## 3. Discussion

### 3.1. X-Ray Crystal Structure of **1** and **2**

A crystalline material was grown in a mixture of DCM/EtOH/Et<sub>2</sub>O at room temperature (r.t.) for 24h. The molecular structure was solved by SHELXS-97 [18,19] software. Crystal data and Ortep (Oak Ridge Thermal-Ellipsoid Plot Program) diagrams of the compounds are shown in Table 1 and Figures 1 and 2, respectively. Selected geometric parameters of compounds **1** and **2** are listed in Tables 2–5.

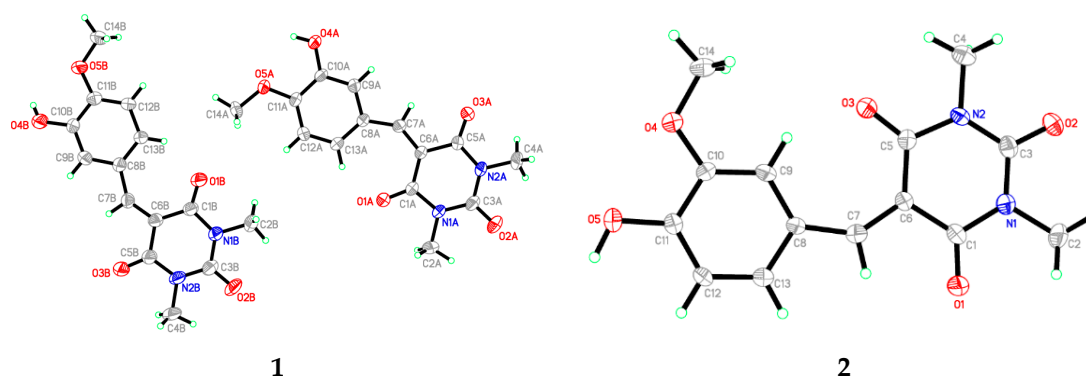
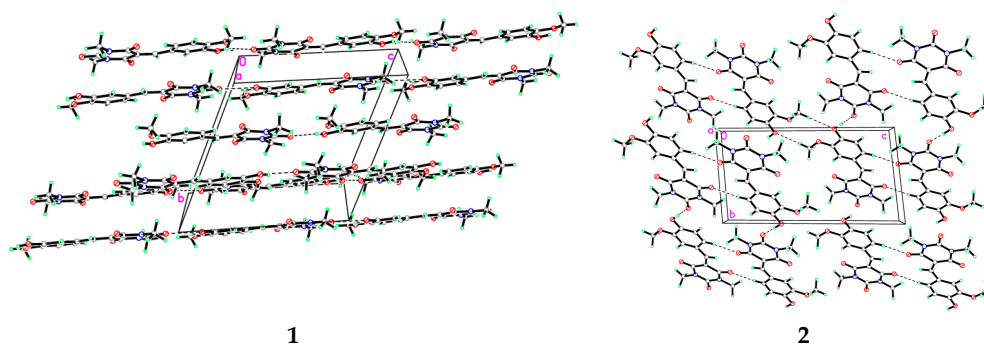


Figure 1. ORTEP (Oak Ridge Thermal-Ellipsoid Plot Program) of the synthesized compound **1** (left) and **2** (right). Displacement ellipsoids are plotted at the 40% probability level for non-H atoms.

**Table 1.** The crystal and experimental data of **1** and **2**.

	<b>1</b>	<b>2</b>
Chemical formula	C <sub>14</sub> H <sub>14</sub> N <sub>2</sub> O <sub>5</sub>	C <sub>14</sub> H <sub>14</sub> N <sub>2</sub> O <sub>5</sub>
M.W	290.27	290.27
T	293 K	296 K
$\lambda$ (Mo K $\alpha$ radiation)	0.71073 Å	0.71073 Å
Crystal system	Triclinic	Triclinic
Space group	<i>P</i> -1	<i>P</i> -1
Unit cell dimensions	<i>a</i> = 9.2265 (10) Å <i>b</i> = 11.9757 (12) Å <i>c</i> = 12.8490 (13) Å $\alpha$ = 110.014 (3)° $\beta$ = 101.912 (3)° $\gamma$ = 90.188 (4)°	<i>a</i> = 5.4539 (4) Å <i>b</i> = 8.1536 (7) Å <i>c</i> = 15.1562 (12) Å $\alpha$ = 83.466 (3)° $\beta$ = 83.950 (3)° $\gamma$ = 79.621 (3)°
Volume	1301.0 (2) Å <sup>3</sup>	656.16 (9) Å <sup>3</sup>
Z	4	2
Density (calculated)	1.482 Mg·m <sup>-3</sup>	1.469 Mg·m <sup>-3</sup>
Absorption coefficient	0.11 mm <sup>-1</sup>	0.11 mm <sup>-1</sup>
F(000)	608	304
Crystal size	0.35 × 0.23 × 0.13 mm	0.19 × 0.13 × 0.08 mm
Theta range for data collection	2.8°–24.9°	2.6°–23.1°
Reflections collected/unique	4554/3207	17059/1475
Completeness to theta = 31.4°	99.9	99.9
Goodness-of-fit on $F^2$	1.08	1.02
Diffractometer	Bruker APEX-II CCD diffractometer	Bruker APEX-II CCD diffractometer
Absorption correction	multi-scan SADABS Bruker 2014	multi-scan SADABS Bruker 2014
$R_{int}$	0.173	0.099
$R(F^2 > 2\sigma(F^2))$	0.088	0.054
wR( $F^2$ ) =	0.252	0.136
$\Delta\rho_{max}/\Delta\rho_{min}$	0.31 and −0.38	0.31 and −0.21
CCDC number	1484809	1484813

**Figure 2.** View of the molecular packing in compounds **1** and **2**. The O–H···O and C–H···O hydrogen bonds are shown as dashed lines.

**Table 2.** Selected geometric parameters (Å, °) of **1**.

O1A–C1A	1.214 (7)	N1A–C2A	1.469 (8)
O2A–C3A	1.207 (6)	N1A–C3A	1.363 (7)
O3A–C5A	1.206 (7)	N1A–C1A	1.403 (6)
O4A–C10A	1.345 (7)	N2A–C4A	1.470 (8)
O5A–C11A	1.360 (7)	N2A–C3A	1.388 (7)
O5A–C14A	1.435 (8)	N2A–C5A	1.389 (6)
O1B–C1B	1.213 (7)	N1B–C3B	1.375 (8)
O2B–C3B	1.209 (6)	N1B–C1B	1.395 (7)
O3B–C5B	1.214 (8)	N1B–C2B	1.465 (9)
O4B–C10B	1.359 (8)	N2B–C4B	1.477 (9)
O5B–C14B	1.431 (9)	N2B–C5B	1.389 (8)
O5B–C11B	1.358 (6)	N2B–C3B	1.365 (8)
C11A–O5A–C14A	118.6 (5)	O3A–C5A–N2A	119.2 (5)
C11B–O5B–C14B	118.0 (5)	N2A–C5A–C6A	117.2 (5)
C1A–N1A–C3A	125.4 (5)	O3A–C5A–C6A	123.6 (5)
C2A–N1A–C3A	116.9 (4)	O4A–C10A–C11A	122.6 (5)
C1A–N1A–C2A	117.7 (5)	O4A–C10A–C9A	117.9 (5)
C3A–N2A–C5A	124.4 (5)	O5A–C11A–C12A	125.1 (5)
C3A–N2A–C4A	116.6 (4)	O5A–C11A–C10A	115.0 (4)
C4A–N2A–C5A	118.9 (5)	O1B–C1B–C6B	125.2 (5)
C1B–N1B–C3B	125.7 (5)	N1B–C1B–C6B	116.2 (5)
C2B–N1B–C3B	116.8 (5)	O1B–C1B–N1B	118.7 (5)
C1B–N1B–C2B	117.5 (5)	O2B–C3B–N2B	121.5 (6)
C3B–N2B–C5B	125.4 (5)	N1B–C3B–N2B	117.3 (4)
C4B–N2B–C5B	117.7 (5)	O2B–C3B–N1B	121.2 (6)
C3B–N2B–C4B	116.9 (5)	O3B–C5B–N2B	119.9 (5)
O1A–C1A–N1A	117.9 (5)	N2B–C5B–C6B	116.8 (5)
N1A–C1A–C6A	116.5 (5)	O3B–C5B–C6B	123.4 (5)
O1A–C1A–C6A	125.6 (5)	O4B–C10B–C9B	118.2 (5)
O2A–C3A–N1A	121.9 (5)	O4B–C10B–C11B	121.8 (5)
O2A–C3A–N2A	120.3 (5)	O5B–C11B–C10B	115.4 (5)
N1A–C3A–N2A	117.8 (4)	O5B–C11B–C12B	124.6 (5)

**Table 3.** Hydrogen-bond geometry (Å, °) of **1**.

D–H...A	D–H	H...A	D...A	D–H...A
O4A–H4OA...O2A <sup>i</sup>	0.87(5)	1.96(5)	2.744(6)	150(4)
O4B–H4OB...O2B <sup>i</sup>	0.70(8)	2.10(9)	2.765(6)	161(11)
C9A–H9AA...O3A <sup>ii</sup>	0.9300	2.5900	3.507(7)	170.00
C13A–H13A...O1A	0.9300	2.1100	2.893(6)	141.00
C13B–H13B...O1B	0.9300	2.0900	2.878 (6)	142.00
C9B–H9BA...O3B <sup>iii</sup>	0.9300	2.5000	3.404 (8)	165.00

Symmetry codes: <sup>i</sup>  $x, y, z + 1$ ; <sup>ii</sup>  $-x, -y + 2, -z + 1$ ; <sup>iii</sup>  $-x + 3, -y + 1, -z + 2$ .**Table 4.** Selected geometric parameters (Å, °) of **2**.

O1–C1	1.218 (4)	N1–C1	1.381 (4)
O2–C3	1.224 (3)	N1–C3	1.367 (4)
O3–C5	1.213 (3)	N1–C2	1.471 (4)
O4–C10	1.363 (3)	N2–C4	1.465 (4)
O4–C14	1.433 (4)	N2–C5	1.399 (4)
O5–C11	1.346 (3)	N2–C3	1.374 (3)
C10–O4–C14	117.4 (2)	O2–C3–N2	121.4 (2)
C1–N1–C3	124.7 (2)	N1–C3–N2	118.2 (2)
C2–N1–C3	117.2 (2)	O2–C3–N1	120.5 (2)
C1–N1–C2	118.1 (2)	O3–C5–N2	118.0 (3)
C3–N2–C5	124.3 (2)	N2–C5–C6	117.1 (2)
C4–N2–C5	118.1 (2)	O3–C5–C6	124.9 (3)
C3–N2–C4	117.6 (2)	O4–C10–C9	125.2 (2)
O1–C1–C6	123.7 (3)	O4–C10–C11	114.3 (2)
N1–C1–C6	117.0 (2)	O5–C11–C10	117.4 (2)
O1–C1–N1	119.4 (3)	O5–C11–C12	123.3 (2)

**Table 5.** Hydrogen-bond geometry (Å, °) of **2**.

<i>D</i> – <i>H</i> ⋯ <i>A</i>	<i>D</i> – <i>H</i>	<i>H</i> ⋯ <i>A</i>	<i>D</i> ⋯ <i>A</i>	<i>D</i> – <i>H</i> ⋯ <i>A</i>
O5–H1O5⋯O2 <sup>i</sup>	0.95 (3)	1.73 (3)	2.679 (3)	178 (3)
C4–H4C⋯O4 <sup>ii</sup>	0.9800	2.5300	3.487 (4)	166.66
C9–H9A⋯O3	0.9500	2.0500	2.855 (4)	141.00
C13–H13A⋯O1 <sup>iii</sup>	0.9500	2.3800	3.320 (3)	172.00
C14–H14A⋯O5 <sup>iv</sup>	0.9800	2.5000	3.482 (4)	175.00

Symmetry codes: <sup>i</sup>  $x + 2, y - 1, z$ ; <sup>ii</sup>  $x - 1, y + 1, z$ ; <sup>iii</sup>  $-x + 1, -y + 1, -z + 2$ ; <sup>iv</sup>  $-x + 2, -y, -z + 1$ .

The 3D chemical structure of the 5-(3-Hydroxy-4-methoxybenzylidene)-1,3-dimethylpyrimidine-2,4,6(1*H*,3*H*,5*H*)-trione; **1** has a pyrimidine-trione ring (C1/N1/C3/N2/C5/C6) and a benzene ring (C8/C9/C10/C11/C12/C13) which are bound together through the exo-double bond C6–C7. The unit cell contains two independent molecules. The dihedral angles between the two rings are 1.38 (3)° and 5.58 (2)° in molecule A and B, respectively. Thus the molecules are nearly planar. Similarly, the 3D chemical structure of the 5-(4-Hydroxy-3-methoxybenzylidene)-1,3-dimethylpyrimidine-2,4,6(1*H*,3*H*,5*H*)-trione **2** was solved. The unit cell contains only one independent molecule and the dihedral angle between the two rings is 2.43 (3)°.

Both **1** and **2** crystallized in space group *P*-1 and the lattice constants are roughly the same in each case. However, there are both similarities and significant differences in the packing modes between the two closely related molecules. The crystal structure of **1** projected along the *c* axis is shown in Figure 2. The molecules are connected by two classical O–H⋯O and two non-classical C–H⋯O hydrogen bonds (Table 3) forming flat sheets. Comparison of the crystal structures reveals that **2** is more loosely packed than **1**. The effective volume of the molecule in **2** estimated by *V*/*Z* is larger by ca 1% than that for **1**. Molecules in compound **2** are packed with one O–H⋯O and three C–H⋯O hydrogen bonds along the *b*, *c* axes (Table 5).

### 3.2. Optimized Structure of **1** and **2**

The optimized structures of the two isomers **1** and **2** are given in Figure 3. Overlay between the optimized and experimental structures are also shown in the same Figure. Tables S1 and S2 (Supplementary Materials) showed the complete list of bond distances and bond angles obtained from the Density functional theory (DFT) calculations and compared with the X-ray results. The results indicated good agreement between the calculated and experimental structures. The correlation coefficients between the calculated and experimental geometrical parameters are 0.988–0.993 and 0.985–0.987 for bond distances and angles, respectively. The maximum bond distance deviations are 0.027 Å (1.95%) and 0.024 Å (1.76%) for compounds **1** and **2**, respectively. Similarly, the bond angles are predicted very well, the maximum percentage errors are 1.86% (2.194°) for **1** and 1.97% (2.312°) for **2**. The small differences between the calculated and experimental geometries are mainly attributed to the known fact that the experimental solid state structure includes intermolecular forces that significantly affect the geometric parameters while the calculated one is a single molecule in the gas phase. It is worth noting that **1** is characterized by an intramolecular O–H⋯O(CH<sub>3</sub>) interaction between the OH group and the neighboring oxygen of the methoxy group where the H–O distance is calculated to be 2.097 Å while the donor-acceptor (O–O) distance is predicted to be 2.650 Å (exp. 2.690 Å). Such H–O interaction was not observed in **2**.

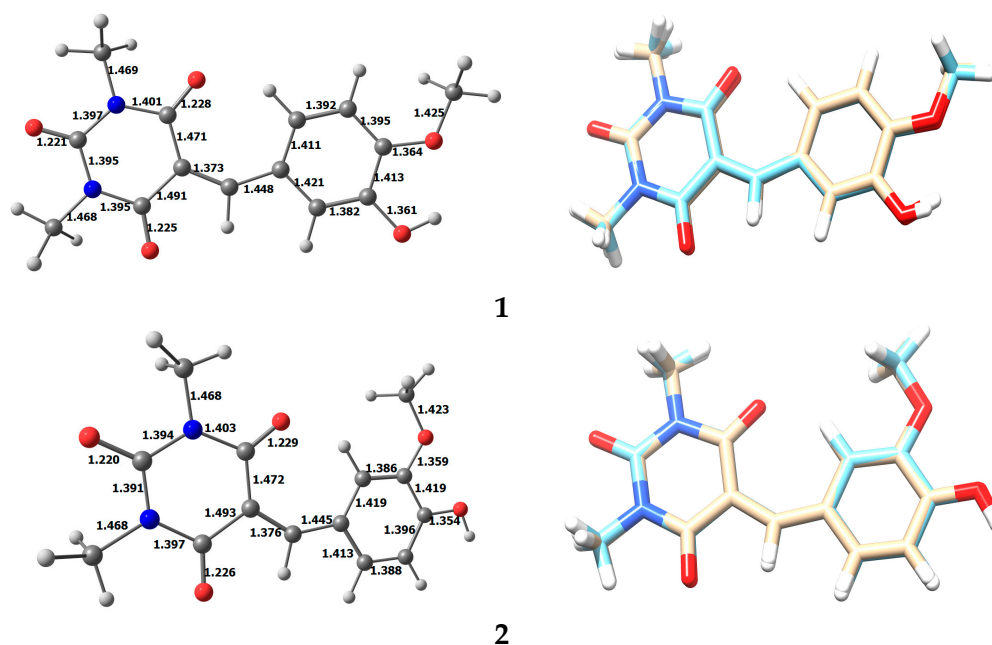


**Figure 3.** The optimized structures (left) and comparative overlay of the calculated and experimental structure (right). Bond distance values are given in Å.

### 3.3. Energy Analysis of the Two Isomers

The total energies ( $E_{\text{tot}}$ ), zero point energy correction (ZPVE) and the corrected total energy ( $E_{\text{corr}}$ ) of the two isomers are given in Table 6. According to these results, isomer **1** is more stable than isomer **2** by 2.56194 Kcal/mol. Also, the thermodynamic parameters such as enthalpy and Gibbs free energy are given in the same table. Based on the Gibbs free energy difference between the two isomers, **1** is thermodynamically more stable than **2**. The extrastability of compound **1** could be attributed to the presence of the intramolecular H–O interaction.

**Table 6.** The total energy ( $E_{\text{tot}}$ ), zero point energy correction (ZPVE), corrected total energy ( $E_{\text{corr}}$ ) and energy difference ( $\Delta E$ ) between the two isomers **1** and **2**.

	<b>1</b>	<b>2</b>
$E_{\text{tot}}$ (a.u)	−1027.5976	−1027.5931
ZPVE (a.u)	0.271445	0.270999
$E_{\text{corr}}$ (a.u)	−1027.3262	−1027.3221
$\Delta E^a$ (Kcal/mol)	−2.5619393	
H (a.u)	−1027.3056	−1027.3013
G (a.u)	−1027.3759	−1027.3734

$$\Delta E^a = E_{\text{corr}}(\mathbf{1}) - E_{\text{corr}}(\mathbf{2}).$$

### 3.4. Frontier Orbital Energy Analysis

The frontier molecular orbitals, HOMO and LUMO are related to the bioactivity of molecules as they give information about their ability to gain or lose electrons. Thus, study on frontier orbital energy can provide useful information about the biological mechanism. The energies of the HOMO and LUMO levels as well as the HOMO-LUMO were obtained from the DFT/B3LYP calculations and the results are listed in Table 7. Compound **1** has lower energy HOMO level than **2**. In contrast, compound **2** has a more stable LUMO level of the lower energy level than that for **1**. Hence **2** is a better electron donor and also a slightly better electron acceptor than **1**. The energy gaps between HOMO and LUMO are 3.57751 and 3.51955 eV for **1** and **2**, respectively. As a result, **1** has a higher energy gap

and is predicted to be more stable towards the electron transport process than **2**. Figure 4 shows the HOMO and LUMO levels of both isomers. The HOMO and LUMO levels are mainly distributed over the  $\pi$ -system of the studied compounds and hence the HOMO-LUMO electron transfer is considered mainly as a  $\pi$ - $\pi^*$  transition.

**Table 7.** The frontier orbital energy (eV) of the studied isomers.

Parameter	1	2
$E_{\text{HOMO}}$	−5.97839	−5.92832
$E_{\text{LUMO}}$	−2.40088	−2.40877
Gap	3.57751	3.51955

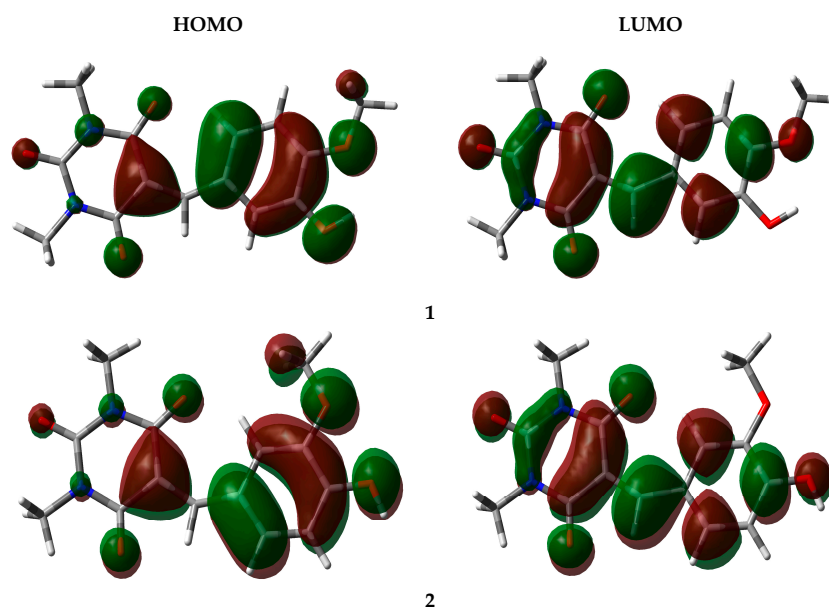


**Figure 4.** The frontier molecular orbitals of the studied isomers.

### 3.5. Natural Atomic Charges ( $Q_N$ ) and Electrostatic Potential (ESP)

Figure 5 exhibits the calculated natural atomic charges ( $Q_N$ ) for all atomic sites. The O and N-atoms have the highest electronegativity and so are expected to have the highest natural charge values. Hence these sites are the most favored to interact with the positively charged receptor active site. In contrast, the OH proton is the most electropositive and is the most favored site to be attached by the negative part of the receptor active sites. The aliphatic carbon atoms are predicted to be more electronegative than the aromatic ones. The ring C-atoms attached to either O or N atoms showed high electropositive character. The most electropositive carbon is the one lying between two N atoms and one O atom. The formation of H-bonding interaction usually affects the charges at the hydrogen, donor and acceptor atoms. It is of note that the charge at the OH proton of **1** is higher than that in **2**. In contrast, its oxygen atom (H-donor) is more electronegative in the former compared to the latter. The acceptor O-atom ( $\text{OCH}_3$ ) in **1** has more negative charge in **1** than **2**. The electrostatic potential (ESP) map shown in Figure 6 indicates that the most reactive electrophilic (blue) and nucleophilic (red) sites are the OH proton and O-atoms in both compounds.

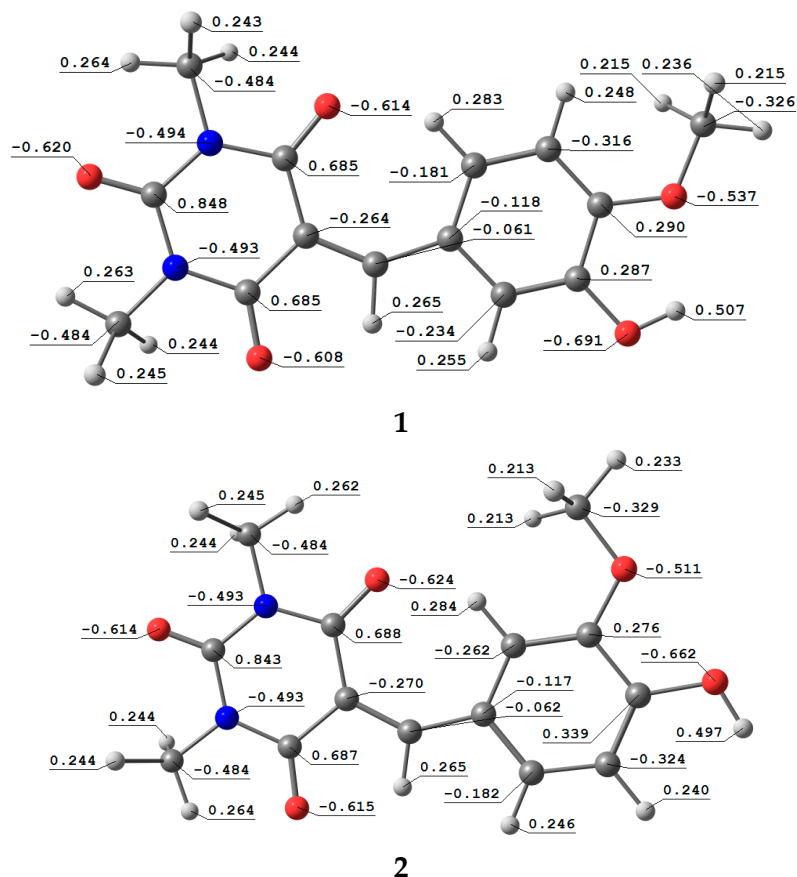


Figure 5. The natural charges at the different atomic sites of compounds 1 and 2.

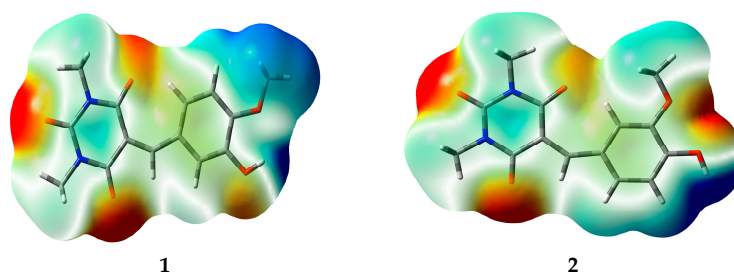


Figure 6. Electrostatic potential (ESP) maps of 1 and 2.

## 4. Materials and Methods

### 4.1. General Remarks

X-ray crystal structure analysis was collected on a Bruker APEX-II D8 Venture area diffractometer (Bruker, Billerica, MA, USA). The NMR spectra were run in deuterated chloroform ( $\text{DMSO-}d_6$ ) using a Jeol-400 NMR spectrometer (Tokyo, Japan).

### 4.2. Procedure for the Synthesis of 1 and 2

A mixture was made of (1 mmol) barbituric acid and (1mmol)3-hydroxy-4-methoxybenzaldehyde (for the synthesis of 1) or 4-hydroxy-3-methoxybenzaldehyde (for the synthesis of 2) in 3 mL of  $\text{H}_2\text{O}$ , and thereaction mixture stirred for 1h. Thereaction was monitored by thin layer chromatography (TLC). After the reaction was complete, the precipitated product was collected by filtration, washed with 2 mL of water, and dried to give the desired compounds 1 and 2. Further crystallization by slow

diffusion of a solution in DCM/EtOH in Et<sub>2</sub>O was carried out to provide a single crystal suitable for X-ray diffraction analysis.

5-(3-Hydroxy-4-methoxybenzylidene)-1,3-dimethylpyrimidine-2,4,6(1H,3H,5H)-trione **1**. (90% yield); M.p. 118 °C; <sup>1</sup>H-NMR (400 MHz, DMSO-*d*<sub>6</sub>) δ: 3.18 & 3.19 (s, 6H, 2NCH<sub>3</sub>), 3.87 (s, 3H, OCH<sub>3</sub>), 7.05 (d, 1H, *J* = 8.8 Hz, C<sub>6</sub>H<sub>3</sub>), 7.69 (dd, 1H, *J* = 8.0 Hz, 1.4 Hz, C<sub>6</sub>H<sub>3</sub>), 8.09 (s, 1H, C<sub>6</sub>H<sub>3</sub>), 8.19 (s, 1H, CH=), 9.88 (s, 1H, OH); <sup>13</sup>C-NMR (100 MHz, DMSO-*d*<sub>6</sub>) δ: 162.7, 160.8, 156.5, 156.4, 153.0, 151.1, 130.5, 125.4, 120.3, 114.8, 111.4, 55.8, 28.9, 28.1; IR (KBr, cm<sup>-1</sup>) ν<sub>max</sub> = 3278, 1680, 1650, 1450, 1250; [Calculated for C<sub>14</sub>H<sub>14</sub>N<sub>2</sub>O<sub>5</sub>: C, 57.93; H, 4.86; N, 9.65; Found: C, 57.92; H, 4.86; N, 9.66]; LC/MS (ESI, *m/z*): [M+], found 290.28, C<sub>14</sub>H<sub>14</sub>N<sub>2</sub>O<sub>5</sub> for 291.28.

5-(4-Hydroxy-3-methoxybenzylidene)-1,3-dimethylpyrimidine-2,4,6(1H,3H,5H)-trione **2**. (88% yield); M.p. 115 °C; <sup>1</sup>H-NMR (400 MHz, DMSO-*d*<sub>6</sub>) δ: 3.27 & 3.22 (s, 6H, 2NCH<sub>3</sub>), 3.83 (s, 3H, OCH<sub>3</sub>), 6.91 (d, 1H, *J* = 8.8 Hz, C<sub>6</sub>H<sub>3</sub>), 7.83 (d, 1H, *J* = 8.8 Hz, C<sub>6</sub>H<sub>3</sub>), 8.28 (s, 1H, C<sub>6</sub>H<sub>3</sub>), 8.33 (s, 1H, CH=), 10.46 (s, 1H, OH); <sup>13</sup>C-NMR (100 MHz, DMSO-*d*<sub>6</sub>) δ: 162.9, 161.1, 156.7, 156.5, 153.2, 151.1, 130.9, 125.8, 120.5, 115.1, 111.9, 55.9, 28.9, 28.6; IR (KBr, cm<sup>-1</sup>) ν<sub>max</sub> = 3278, 1680, 1650, 1450, 1250; [Calculated for C<sub>14</sub>H<sub>14</sub>N<sub>2</sub>O<sub>5</sub>: C, 57.93; H, 4.86; N, 9.65; Found: C, 57.93; H, 4.85; N, 9.67]; LC/MS (ESI, *m/z*): [M+], found 290.28, C<sub>14</sub>H<sub>14</sub>N<sub>2</sub>O<sub>5</sub> for 291.28.

#### 4.3. Theoretical Calculations

The DFT-B3LYP method and the 6-31 G(d, p) basis set in the Gaussian 03 package [20] were used to optimize the structures obtained from the X-ray single crystal structure analysis. Frequency calculations of the optimized structures revealed that the optimized structures are the energy minimum on the potential energy surfaces as no negative frequencies were obtained.

## 5. Conclusions

This section is not mandatory, but can be added to the manuscript if the discussion is unusually long or complex.

**Supplementary Materials:** The following are available online at <http://www.mdpi.com/2073-4352/6/9/110/s1>. Table S1. The calculated bond distances and bond angles compared to the experimental data of **1**; Table S2. The calculated bond distances and bond angles compared to the experimental data of **2**.

**Acknowledgments:** The authors would like to extend their sincere appreciation to the Deanship of Scientific Research at King Saud University for its funding this Research group No. RGP-257-1435-1436.

**Author Contributions:** Assem Barakat conceived and designed the experiments; M. Ali performed the experiments; Abdullah Mohammed Al-Majid and Ayman A. Ghfar analyzed the data; Assem Barakat contributed reagents/materials/analysis tools; Hazem A. Ghabbour carried out the X-ray data collection; Saied M. Soliman carried out the computational studies; Assem Barakat wrote the paper.

**Conflicts of Interest:** The authors declare no conflict of interest.

## References

- Gomez, G.G.; Hutchison, R.B.; Kruse, C.A. Chemo-immunotherapy and chemo-adoptive immunotherapy of cancer. *Cancer Treat. Rev.* **2001**, *27*, 375–402. [[CrossRef](#)] [[PubMed](#)]
- Wang, J.; O'Sullivan, S.; Harmon, S.; Keaveny, R.; Radomski, M.W.; Medina, C.; Gilmer, J.F. Design of barbiturate–nitrate hybrids that inhibit MMP-9 activity and secretion. *J. Med. Chem.* **2012**, *55*, 2154–2162. [[CrossRef](#)] [[PubMed](#)]
- Barakat, A.; Ghabbour, H.A.; Al-Majid, A.M.; Imad, R.; Javaid, K.; Shaikh, N.N.; Yousuf, S.; Choudhary, M.I.; Wadood, A. Synthesis, X-ray crystal structures, biological evaluation, and molecular docking studies of a series of barbiturate derivatives. *J. Chem.* **2016**, *2016*. [[CrossRef](#)]
- Ruble, J.C.; Hurd, A.R.; Johnson, T.A.; Sherry, D.A.; Barbachyn, M.R.; Toogood, P.L.; Bundy, G.L.; Graber, D.R.; Kamilar, G.M. Synthesis of (–)-PNU-286607 by asymmetric cyclization of alkylidene barbiturates. *J. Am. Chem. Soc.* **2009**, *131*, 3991–3997. [[CrossRef](#)] [[PubMed](#)]

5. Andrews, P.R.; Mark, L.C.; Winkler, D.A.; Jones, G.P. Structure-activity relations of convulsant and anticonvulsant barbiturates: A computer-graphic-based pattern-recognition analysis. *J. Med. Chem.* **1983**, *26*, 1223–1229. [[CrossRef](#)] [[PubMed](#)]
6. Xia, G.; Benmohamed, R.; Kim, J.; Arvanites, A.C.; Morimoto, R.I.; Ferrante, R.J.; Kirsch, D.R.; Silverman, R.B. Pyrimidine-2,4,6-trione derivatives and their inhibition of mutant SOD1-dependent protein aggregation. Toward a treatment for amyotrophic lateral sclerosis. *J. Med. Chem.* **2011**, *54*, 2409–2421. [[CrossRef](#)] [[PubMed](#)]
7. Lee, H.; Berezin, M.Y.; Guo, K.; Kao, J.; Achilefu, S. Near-infrared fluorescent pH-sensitive probes via unexpected barbituric acid mediated synthesis. *Org. Lett.* **2008**, *11*, 29–32. [[CrossRef](#)] [[PubMed](#)]
8. McClenaghan, N.D.; Absalon, C.; Bassani, D.M. Facile synthesis of a fullerene-barbituric acid derivative and supramolecular catalysis of its photoinduced dimerization. *J. Am. Chem. C.* **2003**, *125*, 13004–13005. [[CrossRef](#)] [[PubMed](#)]
9. Ivanova, B.B.; Spitteller, M. Possible application of the organic barbiturates as NLO materials. *Cryst. Growth Des.* **2010**, *10*, 2470–2474. [[CrossRef](#)]
10. Wasserscheid, P.; Joni, J. *Handbook of Green Chemistry, Volume 5: Reactions in Water*; Li, C.-J., Ed.; Wiley-VCH Verlag GmbH & Co. KGaA: Weinheim, Germany, 2016.
11. Barakat, A.; Islam, M.S.; Al-Majid, A.M.; Soliman, S.M.; Mabkhot, Y.N.; Al-Othman, Z.A.; Ghabbour, H.A.; Fun, H.K. Synthesis of novel 5-monoalkylbarbiturate derivatives: New access to 1,2-oxazepines. *Tetrahedron Lett.* **2015**, *56*, 6984–6987. [[CrossRef](#)]
12. Barakat, A.; Al-Majid, A.M.; Al-Najjar, H.J.; Mabkhot, Y.N.; Ghabbour, H.A.; Fun, H.K. An efficient and green procedure for synthesis of rhodanine derivatives by aldol-thia-Michael protocol using aqueous diethylamine medium. *RSC Adv.* **2014**, *4*, 4909–4916. [[CrossRef](#)]
13. Al-Majid, A.M.; Barakat, A.; Al-Najjar, H.J.; Mabkhot, Y.N.; Ghabbour, H.A.; Fun, H.K. Tandem Aldol-Michael reactions in aqueous diethylamine medium: A greener and efficient approach to bis-pyrimidine derivatives. *Int. J. Mol. Sci.* **2013**, *14*, 23762–23773. [[CrossRef](#)] [[PubMed](#)]
14. Barakat, A.; Al-Najjar, H.J.; Al-Majid, A.M.; Soliman, S.M.; Mabkhot, Y.N.; Shaik, M.R.; Ghabbour, H.A.; Fun, H.K. Synthesis, NMR, FT-IR, X-ray structural characterization, DFT analysis and isomerism aspects of 5-(2,6-dichlorobenzylidene) pyrimidine-2,4,6(1H,3H,5H)-trione. *Spectrochim. Acta A Mol. Biomol. Spectrosc.* **2015**, *147*, 107–116. [[CrossRef](#)] [[PubMed](#)]
15. Barakat, A.; Al-Najjar, H.J.; Al-Majid, A.M.; Soliman, S.M.; Mabkhot, Y.N.; Ghabbour, H.A.; Fun, H.K. Synthesis and molecular characterization of 5,5'-((2,4-dichlorophenyl) methylene) bis (1,3-dimethylpyrimidine-2,4,6(1H,3H,5H)-trione). *J. Mol. Struct.* **2015**, *1084*, 207–215. [[CrossRef](#)]
16. Al-Najjar, H.J.; Barakat, A.; Al-Majid, A.M.; Mabkhot, Y.N.; Weber, M.; Ghabbour, H.A.; Fun, H.K. A greener, efficient approach to Michael addition of barbituric acid to nitroalkene in aqueous diethylamine medium. *Molecules* **2014**, *19*, 1150–1162. [[CrossRef](#)] [[PubMed](#)]
17. Barakat, A.; Ghabbour, H.A.; Al-Majid, A.M.; El Ashry, E.S.H.; Warad, I.; Fun, H.K. Crystal structure of diethylammonium 5-((4-fluorophenyl)(6-hydroxy-1,3-dimethyl-2,4-dioxo-1,2,3,4-tetrahydropyrimidin-5-yl) methyl)-1,3-dimethyl-2,6-dioxo-1,2,3,6-tetrahydropyrimidin-4-olate, C<sub>23</sub>H<sub>30</sub>N<sub>5</sub>O<sub>6</sub>. *Z. Krist. New Cryst. Struct.* **2016**, *231*, 507–509. [[CrossRef](#)]
18. Sheldrick, G.M. A short history of SHELX. *Acta Cryst.* **2008**, *A64*, 112–122. [[CrossRef](#)] [[PubMed](#)]
19. Sheldrick, G.M. *SHELXTL-PC*; Version 5.1; Siemens Analytical Instruments Inc.: Madison, WI, USA, 1997.
20. Frisch, M.-J.; Trucks, G.-W.; Schlegel, H.-B.; Scuseria, G.-E.; Robb, M.-A.; Cheeseman, J.-R.; Montgomery, J.-A., Jr.; Vreven, T.; Kudin, K.-N.; Burant, J.-C.; et al. *Gaussian 03Revision C.01*; Gaussian Inc.: Wallingford, CT, USA, 2004.

